# Calculation of Scattering Intensities for the Interaction of Light with a Cluster of Dielectric Objects

Emilie Huffman

Department of Physics
Union University

University of Washington REU Program, 2011

# Outline

# Timeline of Theories Regarding Barb Structures

- Any non-iridescent feather coloring was assumed to be caused by pigment. Barbs assumed to be made up of randomly distributed air vacuoles.

Figure: *Coracias Indica*

# Timeline of Theories Regarding Barb Structures

- Any non-iridescent feather coloring was assumed to be caused by pigment. Barbs assumed to be made up of randomly distributed air vacuoles.
- 1935: Raman challenges idea with *Coracias Indica*. Structures hypothesized to be weakly ordered.

Figure: *Coracias Indica*

# Timeline of Theories Regarding Barb Structures

- Any non-iridescent feather coloring was assumed to be caused by pigment. Barbs assumed to be made up of randomly distributed air vacuoles.
- 1935: Raman challenges idea with *Coracias Indica*. Structures hypothesized to be weakly ordered.
- 1940: Idea rejected due to SEM's indication of random structure; revived thirty years later when aspects of random distribution model were falsified.

Figure: *Coracias Indica*

# Prum Enters the Scene

- Conclusive evidence for weak ordering in structure, or *quasi-ordering*, using Fourier analysis of electron micrographs of medullary keratin.

# Prum Enters the Scene

- Conclusive evidence for weak ordering in structure, or *quasi-ordering*, using Fourier analysis of electron micrographs of medullary keratin.
- Successfully predicted wavelengths of optical reflection peak, showing that order in structure *was* responsible for wavelength-specific-colors.

# *Cotinga Cotinga*

- Prum et. al. have studied color production for six avian species, including the *C. Cotinga*, which has barbs which consist of spherical air cavities in a $\beta$-keratin background.

# *Cotinga Cotinga*

- Prum et. al. have studied color production for six avian species, including the *C. Cotinga*, which has barbs which consist of spherical air cavities in a $\beta$-keratin background.
- They have experimentally measured scattering intensity as a function of wavelength, sample orientation, incident light angle, and viewing angle.

# Experimental Results

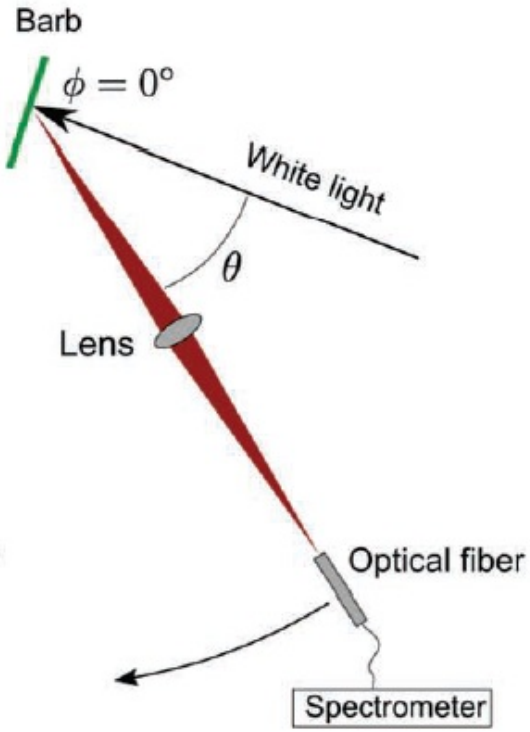


Figure: *The setup for the measurements.*

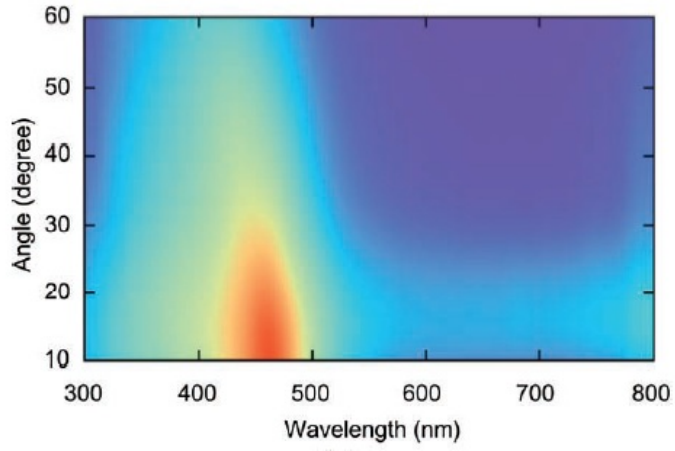


Figure: *Total intensity as a function of wavelength and theta.*

- For directional lighting, the barbs do display iridescence.

# García de Abajo Scattering Model

The electromagnetic field formed from light incident on a grouping of dielectric objects can be written from the Low formalism using scalar longitudinal, magnetic, and electric potentials $\psi_R^L$, $\psi_R^M$, and $\psi_R^E$ as:

$$E = \nabla\psi_R^L + \mathbf{L}_R\psi_R^M - \frac{i}{k}\nabla \times \mathbf{L}_R\psi_R^E \tag{1}$$

where $k = \omega/c$ and $\mathbf{L} = -i(r - \mathbf{R}) \times \nabla$ is the orbital angular momentum operator relative to $\mathbf{R}$, the position vector.
For a system with no nearby external source, $\psi_R^L = 0$. The function $\psi_R^E$ can be obtained using the following identity:

$$\psi_\alpha^E = \frac{i}{k\epsilon_j\mu_j}\frac{1}{L_\alpha^2}(\mathbf{L}_\alpha \times \nabla) \cdot \mathbf{E} \tag{2}$$

Much of the scattering model used was developed by Yoshi Takimoto.

# Scattering Amplitude

For a grouping of dielectrics, $\mathbf{E}$ is equal to $\mathbf{E}^{ext} + \mathbf{E}^{ind}$, where $\mathbf{E}^{ext}$ is the external field and $\mathbf{E}^{int}$ is the field induced by the scattering on the objects. Solving for the induced fields at each position $\mathbf{R}$ yields

$$\mathbf{f}(\Omega) = \sum_{\alpha} e^{-i\mathbf{k}'\cdot\mathbf{r}_\alpha} \sum_{L} \left[ \mathbf{X}_L(\Omega)\, \Psi^{M,ind}_{\alpha,L}/k_0 + \hat{\mathbf{r}} \times \mathbf{X}_L(\Omega)\, \Psi^{E,ind}_{\alpha,L}/k \right] \tag{3}$$

$$\approx \sum_{\alpha} e^{-i\mathbf{k}'\cdot\mathbf{r}_\alpha} \sum_{L} \hat{\mathbf{r}} \times \mathbf{X}_L(\Omega)\, \Psi^{E,ind}_{\alpha,L}/k \tag{4}$$

where $k = \omega/c$ and $\mathbf{X}_L = \mathbf{L}\, Y_L(\Omega)$ is the vector spherical harmonic. The approximation in which the magnetic functions are neglected is made in the electric dipole scattering limit.

# External and Induced Fields

When (1) is inserted into Maxwell's equations, it is found that the scalar functions must satisfy the following wave equation:

$$\left(\nabla^2 + k_j^2\right)\psi = 0 \tag{5}$$

where $k_j = k\sqrt{\epsilon_j \mu_j}$. This implies that the multipole expansion of the electromagnetic field in this region can be expressed as a sum of free spherical waves. The external field can be written in terms of spherical harmonics and spherical bessel functions.
For the system of dielectrics, the electromagnetic field in the medium can be represented as a combination of spherical hankel functions: $h_l^+$ for outgoing waves and $h_l^-$ for incoming waves. Because the sources of $\mathbf{E}^{ind}$ are induced by the external field in the dielectric objects, $\mathbf{E}^{ind}$ is expressed solely in terms of $h_l^+$, the outgoing functions.

# External and Induced Fields

In the linear response approximation for single scattering, the components of the scattered field ($\Psi^{ss}$) are proportional to those of the external field ($\Psi^{ext}$), so the following relationship holds:

$$\Psi^{ind} \approx \Psi^{ss} = t\Psi^{ext} \tag{6}$$

where the factor t is known as the scattering T-matrix. By solving Maxwell's equations in the presence of a dielectric object, using an asymptotic condition that forces $\psi_L$ to equal the sum of the external and induced fields in terms of the t scattering matrix, the elements of such a matrix can be found for each $L$, yielding (for a sphere)

$$t_l^E = \frac{-j_l(\rho_0)\left[\rho_1 j_l(\rho_1)\right]' + \epsilon\left[\rho_0 j_l(\rho_0)\right]' j_l(\rho_1)}{h_l^+(\rho_0)\left[\rho_1 j_l(\rho_1)\right]' - \epsilon\left[\rho_0 h_l^+(\rho_0)\right]' j_l(\rho_1)} \tag{7}$$

where $\rho_0 = ka$ and $\rho_1 = ka\sqrt{\epsilon}$.

# Scattering Intensity Function

The scattering amplitude from a coherent light source incident on a group of $N$ dielectrics can now be expressed as $\sum_{\alpha=1}^{N} \mathbf{f}_\alpha$, where $\mathbf{f}_\alpha$ is given by:

$$\begin{aligned} \mathbf{f}_\alpha(\theta, \phi, \theta_i, \phi_i) &= 4\pi e^{i(\mathbf{k}-\mathbf{k}')\cdot\mathbf{r}_\alpha} \\ &\sum_{l=1}^{\infty}\sum_{m=-l}^{l}\left(\frac{\hat{\mathbf{r}}\times\mathbf{X}_{l,m}(\theta,\phi)}{l(l+1)}\right) \\ &\left[t_{\alpha,l}\mathbf{X}^*_{l,m}(\theta_i,\phi_i)\cdot\frac{\vec{\epsilon}\times\mathbf{k}}{k^2\epsilon_0\mu_0}\right] \end{aligned} \tag{8}$$

# Getting $Chi_{l,m}$

$\mathbf{X}_{l,m}$ is given in spherical polar coordinates ($Y_l^m$ is a spherical harmonic):

$$\mathbf{X}_{l,m} \equiv \hat{\theta}\left\{\frac{-mY_l^m}{[l(l+1)]^{\frac{1}{2}}\, sin\theta}\right\} + \hat{\phi}\left\{\frac{-i}{[l(l+1)]^{\frac{1}{2}}}\frac{\partial Y_l^m}{\partial\theta}\right\} \tag{9}$$

The scattering intensity is then obtained from $\mathbf{f}\cdot\mathbf{f}^*$, where $\mathbf{f} = \sum_{\alpha=1}^{N}$, and $\mathbf{f}_\alpha$ is given by (8).

# Rearranging the Equation

An alternative way of arranging the terms in an equation for the scalar scattering intensity ($\mathbf{f} \cdot \mathbf{f}^*$) is given by the equation below:

$$\mathbf{f} \cdot \mathbf{f}^* = \sum_{\alpha=1}^{N} |\mathbf{f}_\alpha|^2 + \sum_{\alpha \neq \beta}^{N^2-N} \mathbf{f}_\alpha \cdot \mathbf{f}_\beta^* \tag{10}$$

where $\mathbf{f}_i$ is given by (8).

# Coherent and Incoherent Terms

In a randomly distributed assortment of scatterers it can be shown that the terms where $\alpha \neq \beta$ give a negligible contribution to the sum. However, for a large collection of scatterers in some sort of regular distribution the contributions of the terms mixing $\mathbf{f}_\alpha$ and $\mathbf{f}_\beta$, where $\mathbf{r}_\alpha$ and $\mathbf{r}_\beta$ are sufficiently close, become important. Thus the equation becomes:

$$\mathbf{f} \cdot \mathbf{f}^* = \sum_{\alpha=1}^{N} |\mathbf{f}_\alpha|^2 + \sum_{\alpha\beta=\mathrm{nn}} \mathbf{f}_\alpha \cdot \mathbf{f}_\beta^* \tag{11}$$

where “nn" means the near neighbors. The first sum in this equation will yield the same intensities as those for a single sphere multiplied by N, and will be referred to as the incoherent term, whereas the second sum will be referred to as the coherent term, as it contains the structural information of the particular system and creates its distinctive scattering pattern.

# Multiple Scattering

The singly scattered field generated by a dielectric can, in general, be scattered additional times by all other dielectrics in the system. The equation for the induced field thus becomes

$$\psi_\alpha^{ind} = \psi_\alpha^{ss} + t_\alpha \sum_{\alpha \neq \beta} G_{\alpha\beta} \psi_\beta'^{ind} \tag{12}$$

where $G$ is Green's function.
The following recursion relation can be used to solve for the system in question

$$\psi^n = \psi^0 + t \sum G \psi^{n-1}, (n > 0) \tag{13}$$

and Green's function can be approximated using the Rehr-Albers separable approximation.

# Structure Factor

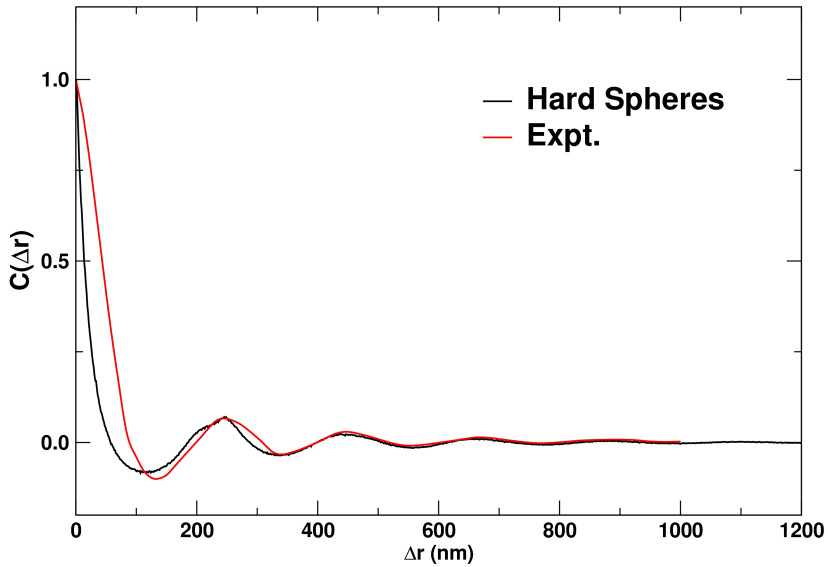


Figure: *Comparison of structure factor for the generated structure to the one found experimentally by Prum et. al. for C. Cotinga.*

- Vila generated Cartesian coordinates for 10,000 spheres distributed in an approximately 5418nm x 5418nm x 5418nm cube.

# Structure Figures

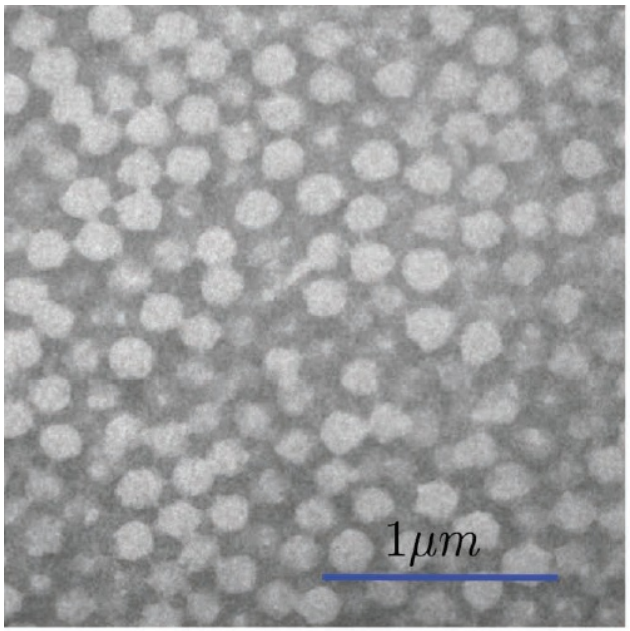


Figure: *TEM image of sphere-type quasi-ordered nanostructures of C. Cotinga. Dark areas are* $\beta$ *—* *keratinandlightareasareair*.

# Structure Figures

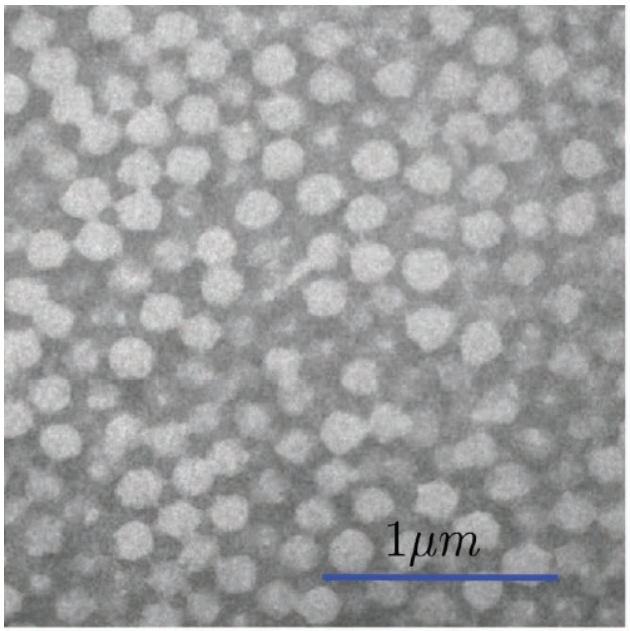


Figure: *TEM image of sphere-type quasi-ordered nanostructures of C. Cotinga. Dark areas are $\beta$ — keratinandlightareasareair.*

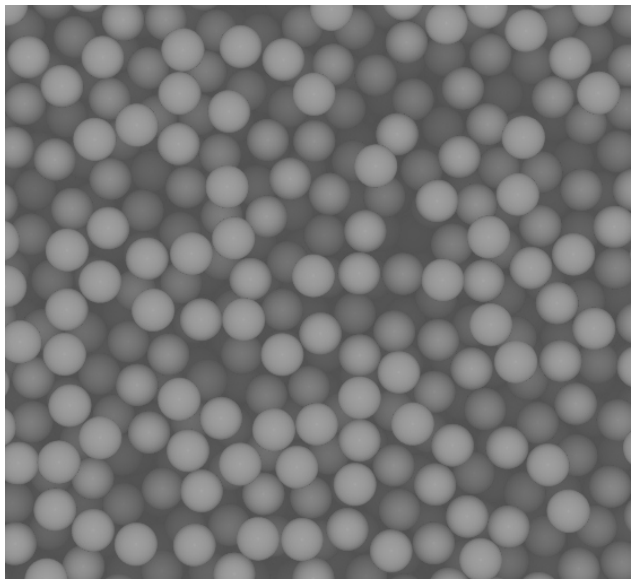

Figure: *Corresponds to a volume fill ratio of 0.5 and depth queueing added to the rendering to mimic the "flatness" of the micrograph.*

# Program

- Written in C.

```
double sphericalBesselY( double x, int n)
{
   return pow( -1, n + 1 ) * sphericalBesselJ( x, - n
}

void sphericalHankelH1( double x, int n, double resul
{
   result[0][0] = sphericalBesselJ( x, n );
   result[0][1] = sphericalBesselY( x, n );
}

void dXSphericalHankelH1( double x, int n, double res
{

   double hankel[1][2] = { { 0.0, 0.0} };
   double hankelMinusOne[1][2] = { { 0.0, 0.0} };
   double hankelPlusOne[1][2] = { { 0.0, 0.0} };

   sphericalHankelH1( x, n, hankel);
   sphericalHankelH1( x, n - 1, hankelMinusOne);
   sphericalHankelH1( x, n + 1, hankelPlusOne);

   result[0][0] = hankel[0][0] + x * ( - ( hankel[0][
```

# Program

- Written in C.
- Reads in coordinates for the 10,000 spheres, and calculates scattering intensities for both the complete single-scattering sum, and for the nearest neigbor approach.

```
double sphericalBesselY( double x, int n)
{
   return pow( -1, n + 1 ) * sphericalBesselJ( x, - n
}

void sphericalHankelH1( double x, int n, double resul
{
   result[0][0] = sphericalBesselJ( x, n );
   result[0][1] = sphericalBesselY( x, n );
}

void dXSphericalHankelH1( double x, int n, double res
{

   double hankel[1][2] = { { 0.0, 0.0} };
   double hankelMinusOne[1][2] = { { 0.0, 0.0} };
   double hankelPlusOne[1][2] = { { 0.0, 0.0} };

   sphericalHankelH1( x, n, hankel);
   sphericalHankelH1( x, n - 1, hankelMinusOne);
   sphericalHankelH1( x, n + 1, hankelPlusOne);

   result[0][0] = hankel[0][0] + x * ( - ( hankel[0][
```

# Program

- Written in C.
- Reads in coordinates for the 10,000 spheres, and calculates scattering intensities for both the complete single-scattering sum, and for the nearest neigbor approach.
- For nearest neighbor approach, only dielectrics located within three dielectric diameter lengths of each other were used in calculation.

```
double sphericalBesselY( double x, int n)
{
   return pow( -1, n + 1 ) * sphericalBesselJ( x, - n
}

void sphericalHankelH1( double x, int n, double resul
{
   result[0][0] = sphericalBesselJ( x, n );
   result[0][1] = sphericalBesselY( x, n );
}

void dXSphericalHankelH1( double x, int n, double res
{

   double hankel[1][2] = { { 0.0, 0.0} };
   double hankelMinusOne[1][2] = { { 0.0, 0.0} };
   double hankelPlusOne[1][2] = { { 0.0, 0.0} };

   sphericalHankelH1( x, n, hankel);
   sphericalHankelH1( x, n - 1, hankelMinusOne);
   sphericalHankelH1( x, n + 1, hankelPlusOne);

   result[0][0] = hankel[0][0] + x * ( - ( hankel[0][
```

# T-Matrix

- The spheres were given a radius of 120 nm, which is the spherical radius for *C. Cotinga*.

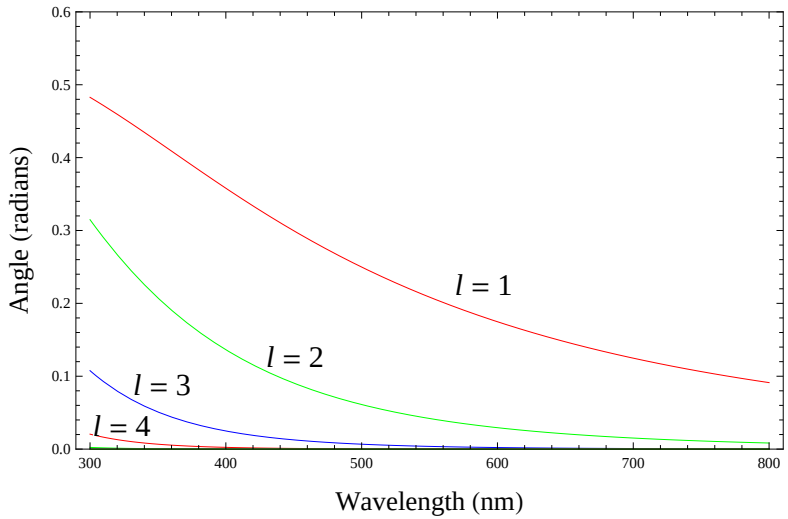


Figure: *The t-matrix as a function of wavelength for values of l ranging from 1-7. As l increases, the t-matrix curves die off.*

# T-Matrix

- The spheres were given a radius of 120 nm, which is the spherical radius for *C. Cotinga*.
- The dielectric constant assigned to the structure was 1.5

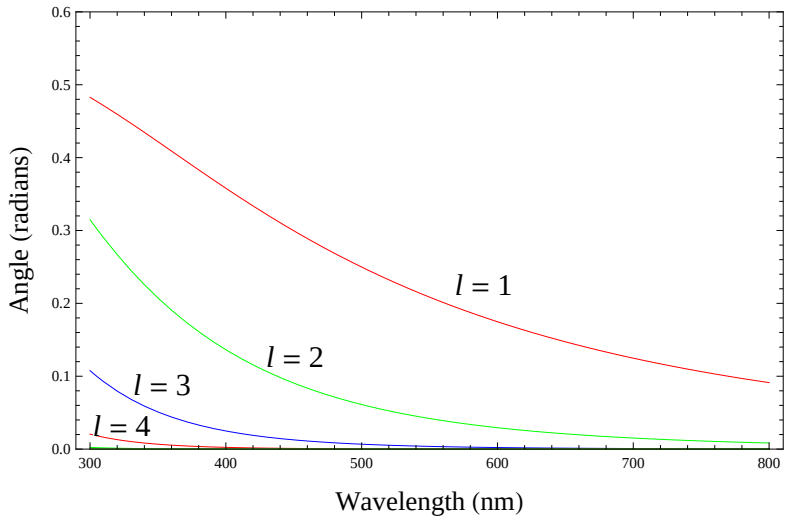


Figure: *The t-matrix as a function of wavelength for values of l ranging from 1-7. As l increases, the t-matrix curves die off.*

# T-Matrix

- The spheres were given a radius of 120 nm, which is the spherical radius for *C. Cotinga*.
- The dielectric constant assigned to the structure was 1.5
- After the fourth term, the t-matrix dies off sufficiently to make any higher l contributions on the scattering sum too minicule to consider. (really, going up to the third term is sufficient...)

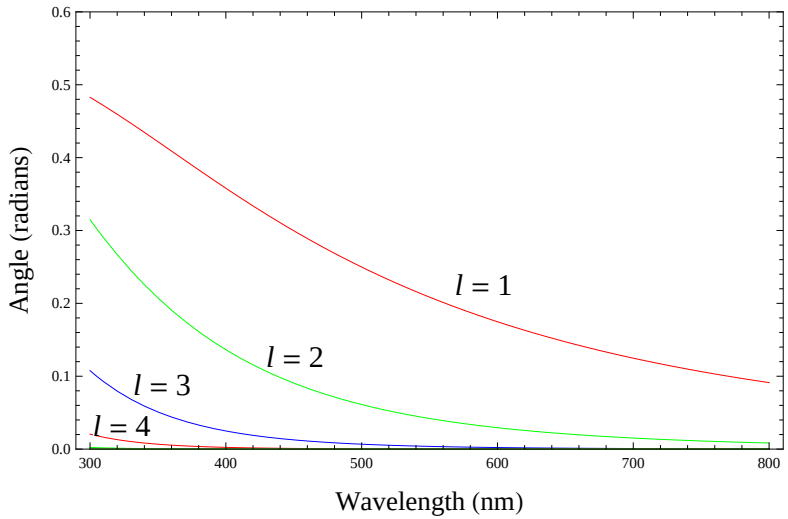


Figure: *The t-matrix as a function of wavelength for values of l ranging from 1-7. As l increases, the t-matrix curves die off.*

# Intensities from Entire Scattering Function

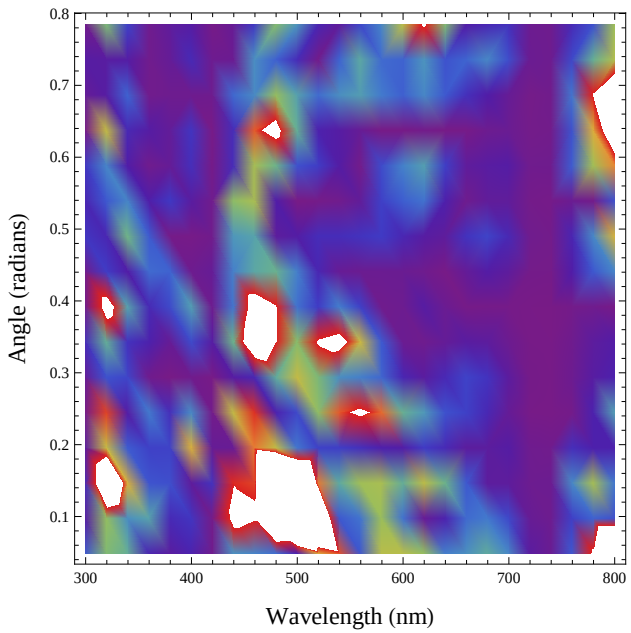


Figure: *For light incident at an angle of $\pi/4$. Has strong intensity for light in the range of 400-500 nm, results consistent with experiment. However, there also appear to be a lot "speckles" or noise.*

- The iridescence suggested by the noise is too strong. It is doubtful that the interactions between the farthest structures in the cell actually contribute, though they are being used in this calculation.

# Intensities from Entire Scattering Function

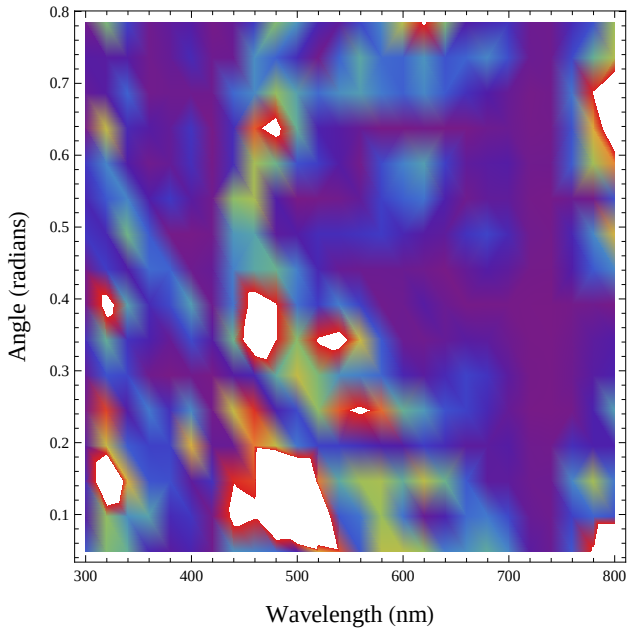


**Figure:** *For light incident at an angle of $\pi/4$. Has strong intensity for light in the range of 400-500 nm, results consistent with experiment. However, there also appear to be a lot "speckles" or noise.*

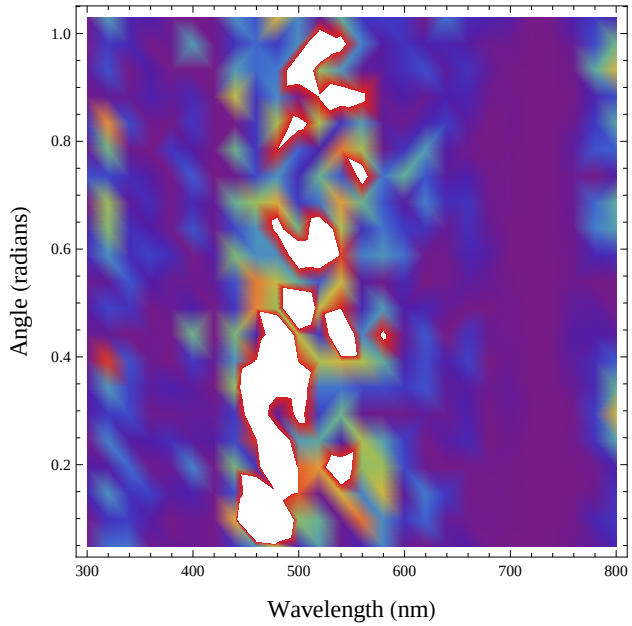


**Figure:** *Gives the scattering intensities for light incident at an angle of $\pi/2$. It also has a strong intensity for light in the range of 400-500 nm, and it can be seen that the "speckles" are still there, but positioned differently.*

- The iridescence suggested by the noise is too strong. It is doubtful that the interactions between the farthest structures in the cell actually contribute, though they are being used in this calculation.

# Intensities from Near Neighbor Approach

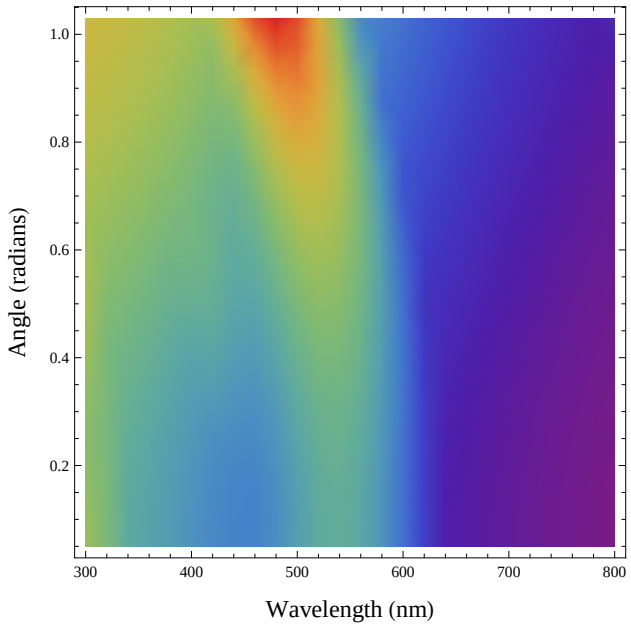


Figure: *Assumes an incident light angle of $\pi/2$ in the theta direction, as well as $\phi = 0$. The highest intensity, is in the higher angle and 400-500 nm range, which is inconsistent with experiment.*

- ...but all “speckles” are gone and more continuity among intensities in images.

# Intensities from Near Neighbor Approach

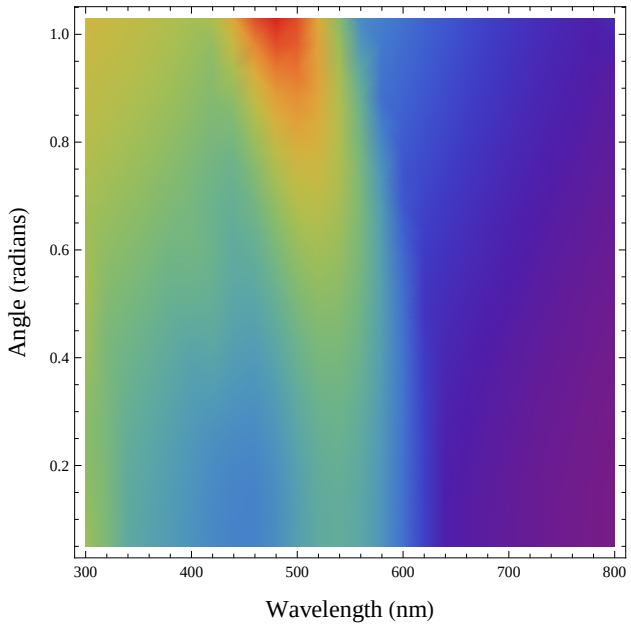


**Figure:** *Assumes an incident light angle of $\pi/2$ in the theta direction, as well as $\phi = 0$. The highest intensity, is in the higher angle and 400-500 nm range, which is inconsistent with experiment.*

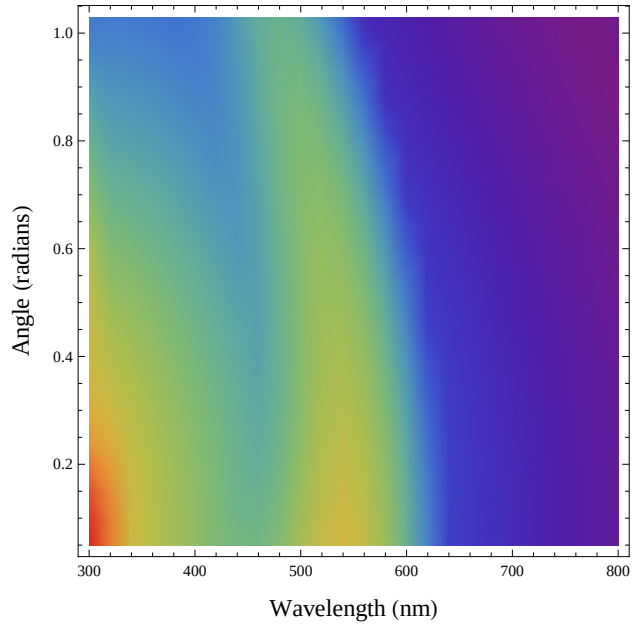


**Figure:** *assumes both an incident angle of $\theta = \pi/2$, and leaving with $\theta = 3\pi/2$. Shows the intensity in terms of a scattered angle phi as well as wavelength. The highest intensity, is in the 500-600 nm range, inconsistent with experiment.*

- ...but all "speckles" are gone and more continuity among intensities in images.

# Experiment and Theory

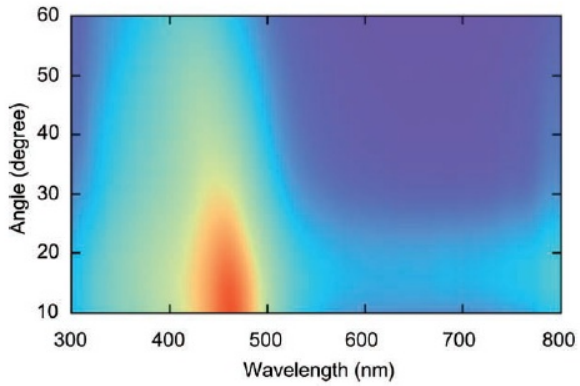


Figure: *The experimental measurements of intensity as a function of wavelength and theta, where theta is the angle between the incident and scattered light.*

- Some problems!

# Experiment and Theory

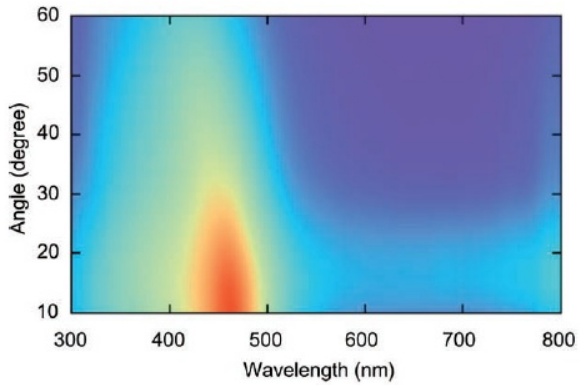


Figure: *The experimental measurements of intensity as a function of wavelength and theta, where theta is the angle between the incident and scattered light.*

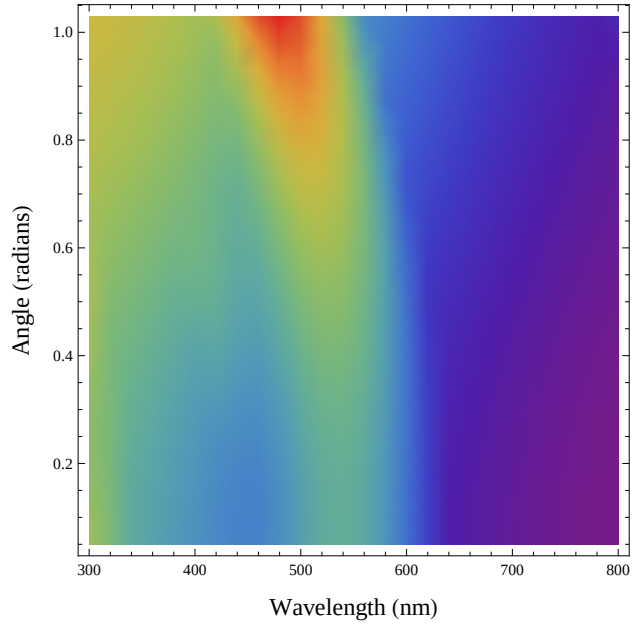


Figure: *The calculated intensities for the same setup.*

- Some problems!

# Summary

- Both attempts to calculate intensity resulted in plots with the strongest intensity in the 400-600 nm range.

# Summary

- Both attempts to calculate intensity resulted in plots with the strongest intensity in the 400-600 nm range.
- All calculations suggest iridescence for directional lighting.

# Summary

- Both attempts to calculate intensity resulted in plots with the strongest intensity in the 400-600 nm range.
- All calculations suggest iridescence for directional lighting.
- All calculations revealed high intensity scattering in distinct visible wavelength ranges, giving a theoretical basis for visible wavelength specific scattering in quasi-ordered structures.

# Summary

- Both attempts to calculate intensity resulted in plots with the strongest intensity in the 400-600 nm range.
- All calculations suggest iridescence for directional lighting.
- All calculations revealed high intensity scattering in distinct visible wavelength ranges, giving a theoretical basis for visible wavelength specific scattering in quasi-ordered structures.

- Future Work
  - Multiple-scattering may be important for modeling this system accurately.
  - Modeling scattering when light is incident from all directions, as it is with daylight. Phi dependence must be removed.

# Acknowledgements


- Advisor
  - John J. Rehr

# Acknowledgements


- Advisor
  - John J. Rehr
- Theory
  - Fernando D. Vila
  - Yoshi Takimoto
  - De Abajo and Low

# Acknowledgements


- Advisor
  - John J. Rehr
- Theory
  - Fernando D. Vila
  - Yoshi Takimoto
  - De Abajo and Low
- Funding
  - UW Physics REU Program funded by NSF PHY-1062795.

# Acknowledgements


- Advisor
  - John J. Rehr
- Theory
  - Fernando D. Vila
  - Yoshi Takimoto
  - De Abajo and Low
- Funding
  - UW Physics REU Program funded by NSF PHY-1062795.
- REU Directors
  - Alejandro Garcia
  - Subhadeep Gupta

# Acknowledgements


- Advisor
  - John J. Rehr
- Theory
  - Fernando D. Vila
  - Yoshi Takimoto
  - De Abajo and Low
- Funding
  - UW Physics REU Program funded by NSF PHY-1062795.
- REU Directors
  - Alejandro Garcia
  - Subhadeep Gupta
- REU Students
  - Gina, Megan, Arman, Charlie, and Micah